JOURNAL OF AGRICULTURAL AND FOOD CHEMISTRY

ARTICLE

pubs.acs.org/JAFC

Permeability of Cork to Gases

David P. Faria,[†] Ana L. Fonseca,[†] Helen Pereira,[‡] and Orlando M. N. D. Teodoro*[,†]

[†]Center for Physics and Technological Research — CEFITEC, Physics Department, Faculty of Sciences and Technology, Universidade Nova de Lisboa, Portugal

[‡]Centro de Estudos Florestais, Instituto Superior de Agronomia, UniversidadeTécnica de Lisboa, Portugal

ABSTRACT: The permeability of gases through uncompressed cork was investigated. More than 100 samples were assessed from different plank qualities to provide a picture of the permeability distribution. A novel technique based on a mass spectrometer leak detector was used to directly measure the helium flow through the central area of small disks 10 mm in diameter and 2 mm thick. The permeability for nitrogen, oxygen, and other gases was measured by the pressure rise technique. Boiled and nonboiled cork samples from different sections were evaluated. An asymmetric frequency distribution ranging 3 orders of magnitude (roughly from 1 to 1000 μmol/(cm·atm·day)) for selected samples without macroscopic defects was found, having a peak below 100 μmol/(cm·atm·day). Correlation was found between density and permeability: higher density samples tend to show lower permeability. However, boiled cork showed a mean lower permeability despite having a lower density. The transport mechanism of gases through cork was also examined. Calculations suggest that gases permeate uncompressed cork mainly through small channels between cells under a molecular flow regime. The diameter of such channels was estimated to be in the range of 100 nm, in agreement with the plasmodesmata size in the cork cell walls.

KEYWORDS: Cork, permeability, gas, density, boiled cork, uncompressed cork

INTRODUCTION

The balance between flexibility and low permeability makes cork a suitable material for sealing purposes. Cork also lasts several years without apparent loss of its sealing performance, and its nontoxicity is well-known. Therefore, it is understandable why it is so largely used in wine closures and sealing gaskets.

Permeability is the property that describes the amount of material (gas or liquid) that flows trough a seal toward the opposite side. Although for many applications permeability as low as possible seems to be preferable, in others some controlled permeation is desired. This seems to be the case in wine bottling, where oxygen permeation through the closure apparently plays an important role in the development of wine, particularly red wine.[1,2] A key debate on this subject was raised in recent years.[3−5] Although consensus seems to be difficult, most authors suggest that the nonnegligible permeation of oxygen through a cork stopper may be a factor of preference for cork over less permeable aluminum screw caps or more permeable synthetic closures.[1] The main routes for oxygen ingress through different closures were addressed by Lopes et al. in ref 6. A very comprehensive review on this subject was recently published by Karbowiak et al.[7]

However, cork has applications other then wine closures.[8] Therefore, permeability is a matter of interest in any application where cork is used because of its suitability as a seal to gases or liquids.

Cork is a cellular material; its cells are hollowed of cytoplasm, being composed of only the cell wall and gas inside. The cell walls' structural components are suberin, lignin, and the polysaccharides cellulose and hemicelluloses. Cork is usually referred to as impermeable, this characteristic being attributed to the suberin, a highly hydrophobic lipid material. Although the inner volume of the cells is basically closed, very small channels (plasmodesmata) between cells were found[9] that might play an important role in the transport of gases through cork.

The cork structure is similar to a hive, in which the cells resemble a prism with an average of six sides, oriented according to the tree radius. Cork has several major inhomogeneities such as large pores and channels, most of them parallel to the tree radius and well visible macroscopically.[10]

The aim of this work was to provide a comprehensive characterization of the permeability to gases of this alveolar material in the absence of compression. We performed permeability measurements for different qualities of cork with and without the boiling treatment used in the manufacturing industry for the preparation of raw cork material used in the production of wine stoppers. We also performed measurements in the three different sections to evaluate the permeability anisotropy. Moreover, the use of different gases in this work, therefore varying the permeant mass, provided an understanding of the transport mechanism of gases through cork.

However, the goal of this work was not to study cork as a closure in real conditions as, for instance, in wine stoppers. We intended to characterize the permeability of cork as a natural material, without compression, and to get some insight into the transport mechanisms of gases under such conditions. The basic idea was to determine how and to what extent the bark cell walls are permeable to gases. In other experiments we measured the effect of compression on the permeation and characterized the permeation of liquids and vapors through cork. Moreover, the total permeation of cork stoppers in bottlenecks was also studied using the technique described here.

All studies found on the permeability of cork were performed using oxygen with the purpose of characterizing cork as a wine

Received: February 4, 2011
Revised: March 24, 2011
Accepted: March 24, 2011
Published: March 24, 2011

Table 1. Sample description Summary

plank treatment	nonboiled	boiled
no. of samples	38	69
sampled sections	radial, transverse, and tangential	
plank thickness (mm)	type 3 = 42 ± 5	type 3B = 48 ± 5
	type 2 = 33 ± 4	type 2B = 38 ± 4
	type 1 = 17 ± 3	type 1B = 18 ± 3
sample dimensions	disks of ≈2 mm thick and 10 mm diameter	
permeation area	9.6 mm^2 (∅ 3.5 mm)	

closure. Therefore, cork stoppers were used, fitted in bottles or bottle-like conditions. Such studies were done using the Mocon method or by an especially developed colorimetric method.[11] One of the main drawbacks of these methods is the long time required to achieve a steady state and, therefore, stable measurements.[12] Those studies are well summarized in refs 7 and 13 and were always performed on cork stoppers fitted in bottles or bottle-like conditions. For that reason it is difficult to get insight into the permeability of cork in the absence of compression. Moreover, the influence of the orientation on the cork section was not studied in any of those works (stoppers are always cut across the same section).

In this work, we used a helium mass spectrometer leak detector to measure the gas flow. This equipment provides a direct measurement of He flow rate in a very wide range (≈10 orders of magnitude). Furthermore, the measurements provided by the leak detector are easily traceable, using calibrated reference leaks. These leaks can be purchased in a wide range of values, well below (and above) the values we found. However, this type of detector is suitable only for helium. For that reason, measurements with other gases were few and performed according to the standard pressure rise method commonly used to measure the permeability of plastics.[14,15] The mass spectrometer leak detector allowed measurement of the permeability of more than 100 samples, and the pressure rise technique revealed a relationship between the permeation for helium and the permeation for other gases such as nitrogen and oxygen.

EXPERIMENTAL PROCEDURES

Sampling. The permeability was measured in selected cork samples without macroscopic defects. Some of these natural defects are large pores or channels through which the gas flow has almost no restrictions and may lead to unmeaningful results regarding the true permeability of the cork cell tissue. Moreover, because we were dealing with a natural product, a large variability of results was expected.

This was minimized using small-sized samples where we could easily find a quasi-homogeneous and defect-free spot of a few millimeters in diameter.

Samples were taken from planks of reproduction cork with a 9-year production cycle. The three plank thickness classes of 22−27 mm (thin), 27−32 mm (half-standard), and 32−40 mm (standard) were sampled, coded as types 1, 2, and 3, respectively, which correspond to different average annual cork growths (Table 1). These planks are the raw material used in the production of wine stoppers (types 2 and 3) or of disks for composite stoppers, that is, for sparkling wines (type 1).[10]

The planks were subdivided, and one part was treated by immersion in boiling water during 1 h. This is the usual preprocessing step that the raw cork planks undergo industrially.[5] This boiling process typically expands the plank volume, predominantly increasing the plank thickness by about 15% and releasing residual stresses in the cell walls.[8] The letter "B" refers to the boiled cork samples.

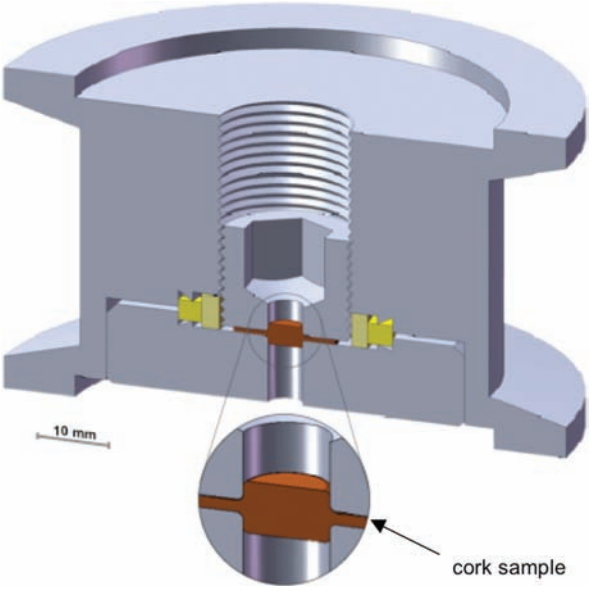

Figure 1. Cork sample compressed between two flat stainless steel surfaces. The permeation area was 3.5 mm in diameter.

Cylinders of 10 mm diameter were cut from the planks along the three main axes in relation to the tree stem (axial, radial, and tangential). Then, cylinders were sliced in disks about 2 mm thick. Finally, a visual inspection was performed to select samples without visible defects in a central area of approximately 3 mm in diameter. Sample rejection was between 50 and 80% or even more in the case of radial sections. Table 1 summarizes the details of the analyzed samples. Prior to testing, every sample was weighed and its thickness measured.

Designation of the cork disk sections follows the usual nomenclature in plant anatomy and cork studies:[5] a transverse section is perpendicular to the axial tree direction, a tangential section is perpendicular to a tree radial direction, and a radial section contains a tree radius and the vertical axis. Cork stoppers are cut from the transverse section.

Methods. Samples were mounted on a specially made sample holder illustrated in Figure 1. The cork disk was wedged between the holder body and a screwable cylinder, both having a drilled aperture of 3.5 mm in diameter. The lower part of the holder was replaceable, allowing easy modification of the sampled area (together with the screwable cylinder). This lower piece was built on a standard CF16 flange sealed with a copper gasket as used in ultrahigh-vacuum systems. The holder was fitted with two standard KF40 flanges for quick assembling and disassembling in the leak detector and gas filling system.

The sample holder was leak tested with a thick neoprene disk, and no leaks were detected ($<10^{-10}$ cm^3 (STP)/s).

Efforts were made to ensure that every sample was well sealed between the two surfaces and the gas flowed through the sampled area. Samples were tested with different torques applied to the upper cylinder. Above a torque of ≈1 N m, no change in the flow was detected. We assumed that in such conditions the gas flow was mainly due to permeation. Thereafter, all samples were tightened with a torque well above the aforementioned limit, but below the point of sample destruction (however, every tested sample was permanently modified). The transition area between the compressed and uncompressed sample parts was disregarded and included the sampled area.

The sample holder was mounted directly on the leak detector. The upper flange was fitted to a gas filling system. The upper volume was pumped down to pressures below 1 mbar and then filled with pure (99.99%) helium to a monitored pressure of 1.0 atm. The leak detector was switched on before gas filling and connected to a computer for

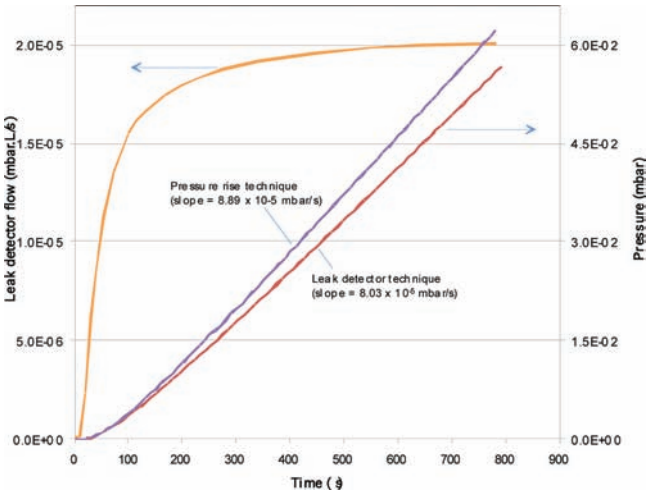

Figure 2. Method validation. The graph shows the He flow as acquired by the leak detector (left scale) and its comparison after integration in time with the pressure rise technique (right scale); the difference lies within the uncertainty of the reference leaks used. This example shows the larger difference found among tests; the arrows indicate the corresponding axis of the plotted lines.

continuous acquisition (every second). Typical acquisition time was about 1 h per sample.

A modern leak detector, type ASM 142 from Adixen, was used. This detector is fully automated and has an internal reference leak for periodic calibration. This reference leak has temperature correction and was calibrated externally in our ISO/IEC 17025:2005 accredited laboratory with an uncertainty of 10% ($k = 2$).

For the pressure rise method, the same holder was used. The lower side was connected to a high-vacuum system via a valve. Prior to pumping, the holder and fittings (without sample) were baked for more then 10 h at temperatures above 80 °C under vacuum to ensure proper degassing. After cooling and with a disk of negligible permeability, the pressure rise was monitored to evaluate the contribution of residual degassing to the pressure.

Then the sample was assembled, the lower volume was evacuated to a pressure below 10^{-5} mbar, and the valve was closed. The upper volume was filled with the testing gas in a procedure similar to that used with the leak detector. The pressure in the lower volume was monitored with a high-accuracy pressure gauge (MKS 690A Baratron) for a time long enough to have a constant slope pressure increase (typically a few hours).

Because the sample was exposed to vacuum well below the water vapor pressure (≈0.1 mbar) in all measurements, it was considered void of water. This is a limitation of the technique that cannot be overcome (controlled relative humidity is not possible).

The volumetric gas flow rate, Q, is given by the relationship (for constant volume)

$$Q = V\frac{dp}{dt}$$

where p is the pressure, V the closed volume, and t the time. Therefore, the volume has to be known. It was measured fitting an extra (known) volume via a valve and producing an adiabatic expansion (or compression). The initial and final pressure was measured, and the volume was then calculated with an estimated uncertainty of better than 5%. All measurements were done at room temperature.

One of the experimental concerns within the framework of this study was to demonstrate that the value read by the leak detector would be the same as that acquired from the pressure rise technique. Therefore, we measured the permeability for He in the same sample using both methods to achieve method validation. Figure 2 shows the results for

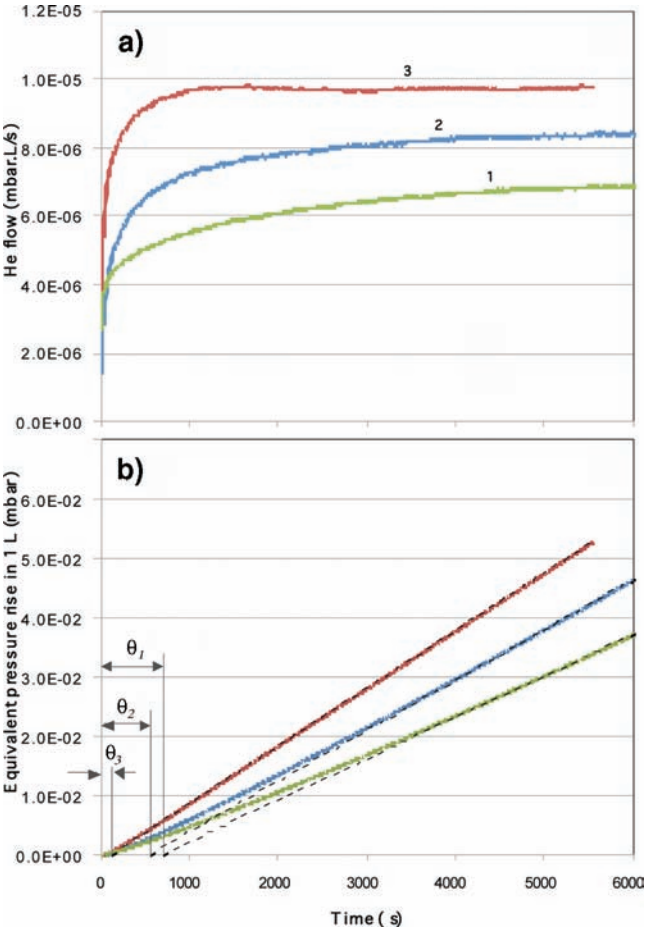

Figure 3. (a) Three typical He permeation measurements as acquired by the leak detector; (b) same as (a) but converted to the equivalent pressure rise in 1 L volume. Note the differences in time lag. $\theta_1 = 678$ s; $\theta_2 = 536$ s; $\theta_3 = 107$ s.

the worst of three samples for which we did this comparison. Even in the worst case, the difference in the slope lies well within the uncertainty of the reference leak.

Calculations. All measurements were acquired in terms of volumetric gas flow rate and thereafter converted to permeability. Considering volumes at standard temperature and pressure (STP), the following conversion may be convenient for flow rate units:

$$1 \text{ mbar·L/s} \approx 1 \text{ mL (STP)/s}$$

Permeability (Pe) was calculated from the measured flow rate (Q) by taking into account the thickness of the sample d, the permeation area A, and the testing pressure difference Δp_t, by the following relationship:

$$\text{Pe} = \frac{Q \times d}{A \times \Delta p_t}$$

For convenience, the permeability was converted to what seemed a better-suited unit, μmol/(cm·atm·day): 1 μmol/(cm·atm·day) is the total amount of gas flow through a section of 1 cm^2 and 1 cm thick under a pressure difference of 1 atm after 1 day. A temperature of 300 K was used in the conversion calculations.

RESULTS

Figure 3 illustrates typical results for three different samples acquired by the leak detector. The He flow was well within the

measuring range of the leak detector in the "fine" mode (10^{-4}–10^{-11} mbar·L/s). The permeated flow starts very small and then increases to a steady state value. Sample 1 was from plank 2B with a tangential section, sample 2 from plank 3B with radial section, and sample 3 from plank 3. The corresponding permeabilities are in the inset of Figure 3.

The time needed to get a constant value can be described by the so-called time lag obtained by the intersection of the tangent with the time axis when a constant slope is achieved, as shown in Figure.3b. In those samples the time lags were θ_1 = 678 s, θ_2 = 536 s, and θ_3 = 107 s.

Although the flow rate of these three samples was of the same order of magnitude, they could range up to 3 orders as shown by Figures 4–6. In Figure 4 the mean permeability is plotted for every plank class. We note that samples from thinner planks on average permeate less than those from thicker planks. The mean permeability for plank 1B is 10 times lower than samples from plank 3 (or 3B). Also, it is clear that the boiling process reduces the mean permeability.

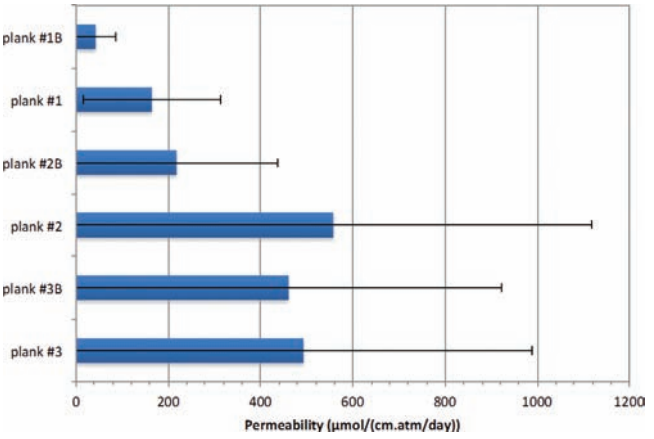

Figure 4. Mean permeability and standard deviation for samples from different planks. The variability is so large that the standard deviation is larger than the average in five of six classes.

Figure 4 also plots the standard deviation for those classes. Although the permeability axis is in a log scale, it can be noted that standard deviations are larger than average for almost all classes. Only class 1 shows a lower value, but it is also the class with less population (only nine samples). This huge standard deviation suggests that the distribution of this property under study is not normal and, therefore, the standard deviation has no meaning in this case.

No systematic difference was found among sections. Any eventual small difference was hindered by the high dispersion of results.

The frequency distribution for all sample types is shown in Figure 5. To minimize the effect of a limited number of samples, the results were grouped in permeability classes of increasing ranges. The left scale refers to the frequency density, and the right scale provides an idea of the cumulative probability.

The permeability values range >3 orders of magnitude (see Table 2). The distribution displays a clear peak at very low values (<100 μmol/(cm·atm·day)), but also makes a significant contribution at much higher values. This behavior is similar to the known γ distribution used in statistics. However, in our case the contribution at high values seems to be more significant than in γ distributions.

The difference between boiled and nonboiled samples is perceptible in Figure 5. Almost 40% of the boiled samples have permeabilities of <100 μmol/(cm·atm·day), whereas in the case of nonboiled samples only 7% are in the same set. The contribution at higher values is more noticeable for nonboiled samples.

The 95% percentile provides a useful figure for permeability. It describes the number below which we have 95% probability of having the permeability of a sample. The 95% percentile is 670 μmol/cm/day for boiled cork, but it is more than double this

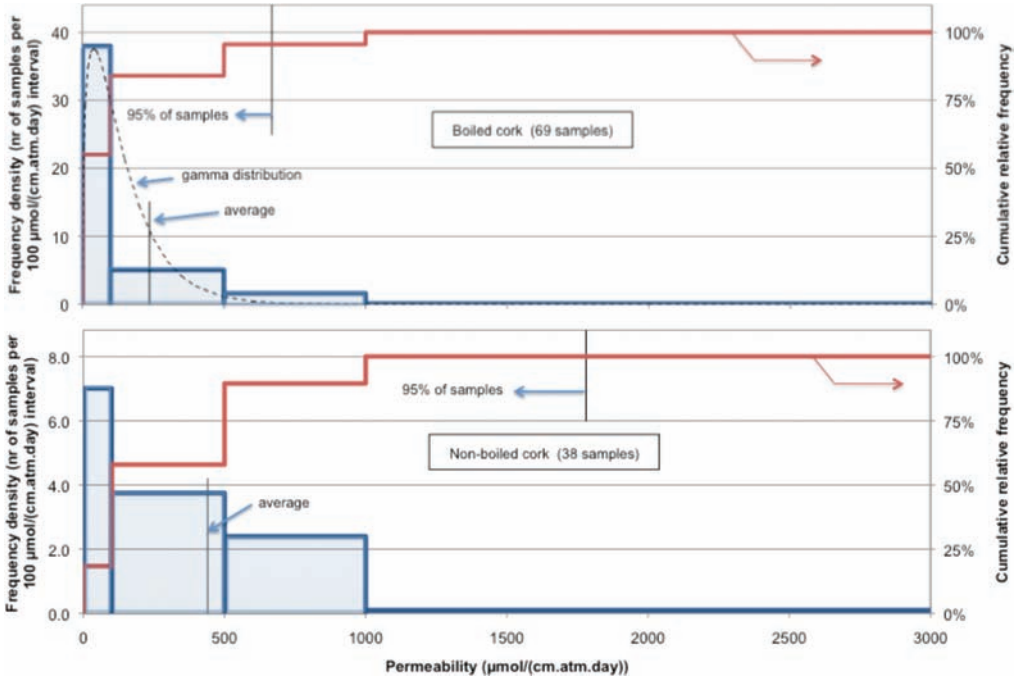

Figure 5. Distribution of permeabilities for boiled and nonboiled samples. Boiled samples show lower permeabilities. Note the position of average and 95% percentile. The upper distribution shows the similarity with a γ distribution.

dx.doi.org/10.1021/jf200491t |J. Agric. Food Chem. 2011, 59, 3590–3597

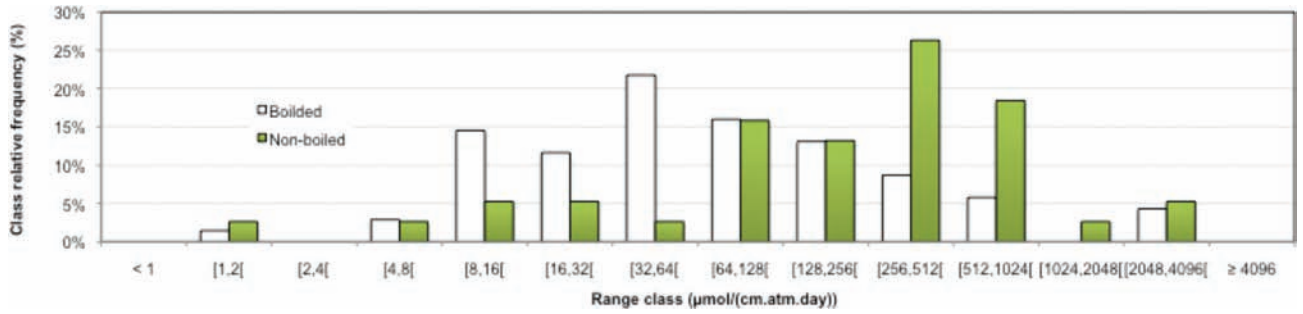

Figure 6. Frequency histogram of permeability. Class ranges were chosen to span constant log intervals.

value for nonboiled samples. However, it is >1 order of magnitude higher than the decade mode (Table 2).

A closer look at the frequency distribution can be done if data are grouped as shown in Figure 6. Note that classes now have continuously duplicated permeability widths. The huge range of values is evident. Also, the difference between the two sets of samples and the significant contribution at values well above average and above the mode are again clear.

The permeability was also measured for nitrogen, oxygen, carbon dioxide, and tetrafluoroethane (R-134a, refrigerant gas) using the pressure rise technique. These experiments were done on the same sample to avoid sample variability. The measurements were performed a minimum of three times per gas type. The result is represented in Figure 7.

The permeability for heavier gases is considerably lower, as expected. The ratio of Q_{N2}/Q_{He} is 0.36, and Q_{O2}/Q_{He} is 0.32. These ratios may be used to convert all of the permeabilities measured for helium to permeabilities for nitrogen or for oxygen. Therefore, the scales in Figures 4 and 5 can be converted to describe the permeation for these gases. The permeation is roughly one-third of that for He.

DISCUSSION

One of the main findings in this work is the outstanding variability of cork permeability, even in the absence of macroscopic inhomogeneities. Although the boiled cork samples show a higher proportion at low values, in both cases permeability ranges 3 orders of magnitude. This result suggests that such cork samples are still quite inhomogeneous.

A similar large variability was also noted by other authors (see, for example, refs 7 and 16 and references cited therein). As stated before, all published data concerning permeability are related to the permeance of oxygen through compressed cork as in a wine closure. From the permeance data one can infer the permeability by taking the typical closure dimensions, 44 mm long and 18.5 mm in diameter (in the bottleneck).

Godden et al., using the Mocon technique, measured a thousand-fold variation ranging 0.0001 to 0.1227 mL/day/closure (0.05−64 mg/year/closure) in 12 samples 3 years after bottling.[17] Lopes et al. used an improved colorimetric method to measure the oxygen ingress into the bottle under conditions similar to those of wine bottling. For natural cork closures he found values between 0.24 ± 0.16 and 0.50 ± 0.30 mg/L/month (10 times variation) in 16 samples fitted in bottles of 0.35 L.[18] In a different work, the same authors studied the kinetics of the oxygen ingress over time as a function of the bottle storage position (vertical or horizontal).[19] In vertical position they measured rates ranging from 0.1 to 2.7 μL/day (27 times variation) in 8 samples of 2 different types of cork over a period between 2 and 12 months after bottling. In another paper, Hart cites a work performed by Southcorp Wines in which the oxygen permeation of 35 closures was assessed, displaying high variability ranging from <0.001 to 1.0 mL/day.[20] Silva et al., in a study comparing the performance of synthetic and natural closures, found an oxygen transmission rate of 0.078−0.083 mL/stopper/day for one-piece cork stoppers.[21]

Data from these studies were converted to permeabilities and compared with our data in Figure 8. Our results overlap 2 orders of magnitude data from other authors and have a similar thousand-fold variation. However, our work shows that uncompressed and dry cork has about 10 times higher permeability. This is reasonable because compression should partially close flow paths, therefore increasing flow resistance.

No correlation was found between the sample section and permeability. However, it was much more difficult to find "good" samples with tangential sections because most defects are across this plane. This is why cork stoppers are always drilled to keep such defects perpendicular to the stopper cylindrical axis.[10]

From Table 1 we note that boiling typically reduces cork density. When boiled, cork samples increase their volume, mostly through expansion in the radial direction.[22] This suggests that permeability may correlate with sample density. This is plotted in Figure 9 for all samples grouped as shown in Figure 4. Boiled samples are indeed less dense and, for both sets (boiled and nonboiled), the higher the density, the lower the mean permeability.

Thinner planks possess typically higher densities, and the thinner plank 1 shows the lowest mean permeability. It was shown that in thin planks there is a higher proportion of smaller cells and thicker cell walls.[23] Therefore, more cell walls are present, which increases the barrier reducing the gas flow. Consequently, it is understandable why such samples showed lower permeability.

In natural cork the cell walls are corrugated due to growth stresses.[23] Under boiling, walls release their stress, partially returning to their original volume. This explains the cell expansion and the lower density of such samples, but not the observed decrease in the mean permeability. The reason behind this requires further research because it seems that boiling also affects the gas permeation paths.

Therefore, it is important to understand the permeation mechanism through cork. Data in Figure 7 are fitted with a function that describes the molecular regime of flow in very thin channels or capillaries. This flow occurs when the mean free path of the molecules is higher than the channel diameter.[24] The molecular flow rate, Q_{mol}, was calculated by Knudsen as

$$Q_{mol} = a\left(\frac{T}{M}\right)^{1/2}\frac{D^3}{L}\Delta p_t$$

where a is a constant, T the gas temperature, M the molecular mass,

Table 2. Data Analysis Summary[a]

	plank 1			plank 2			plank 3			plank 1 (boiled)			plank 2 (boiled)			plank 3 (boiled)		
	radial	tangential	transversal	radial	tangential	transversal	radial	tangential	transversal	radial	tangential	transversal	radial	tangential	transversal	radial	tangential	transversal
no. of samples	5	5	5	5	4	5	5	0	4	6	5	5	15	15	8	5	5	5
mean permeability[b]	359.2	1385.8	273.3	605.0	304.1	1281.4	228.3		217.7	1207.9	174.6	385.7	76.7	218.1	859.9	35.4	89.2	50.8
standard deviation[b]	403.2	1424.3	343.8	182.6	338.0	1180.7	253.7		157.0	1460.5	176.4	237.5	61.6	292.5	1543.5	31.0	123.6	39.4
overall mean permeability[b]	440 (147)									237 (79)								
overall standard deviation[b]	585 (195)									551 (184)								
permeability range[b]	1.1−2522 (0.4−841)									1.8−3404 (0.6−1135)								
mode (decade)[b]	70−80 (23−27)									10−20 (3−7)								
95% percentile[b]	1780 (593)									670 (223)								

[a] Data displayed in parentheses are corrected for oxygen by the ratio derived from Figure 5. [b] Units in μmol/(cm·atm·day).

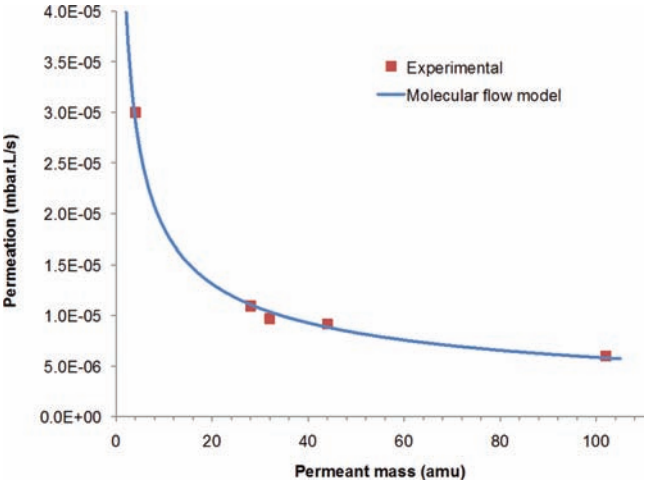

Figure 7. Permeation through cork follows the model for molecular gas flow in porous media. The pressure rise technique was used to measure the flow of He, N_2, and O_2 through the same sample.

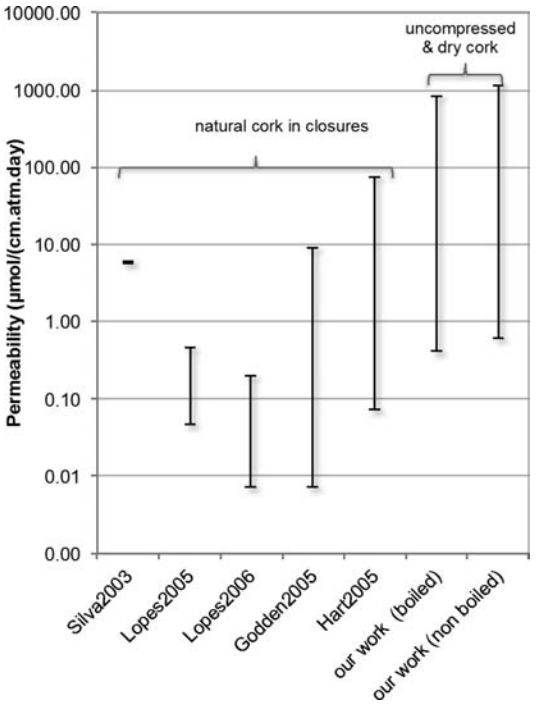

Figure 8. Comparison of the equivalent oxygen permeability with data from other authors. A closure 44 mm long and 18.5 mm in diameter was considered to derive the permeability from the oxygen transmission rate published in the following references: Silva,[21] Lopes,[18] Lopes,[19] Godden,[17] and Hart[20] With the exception of the Lopes data, the permeability was measured under dry conditions. Lopes data were obtained under conditions similar to those of wine aging.

D the channel diameter, and L the channel length; Δp_t is the pressure difference between the channel entrance and exit.

The fit in Figure 7 considers mass M to be the only variable, all the rest being fitting parameters. The high correlation suggests that we are indeed in the presence of this kind of flow, which is typical of porous membranes and well described in the literature.

Therefore, the transport of gas through cork seems to be done mainly via small channels across the cell walls. The size of these

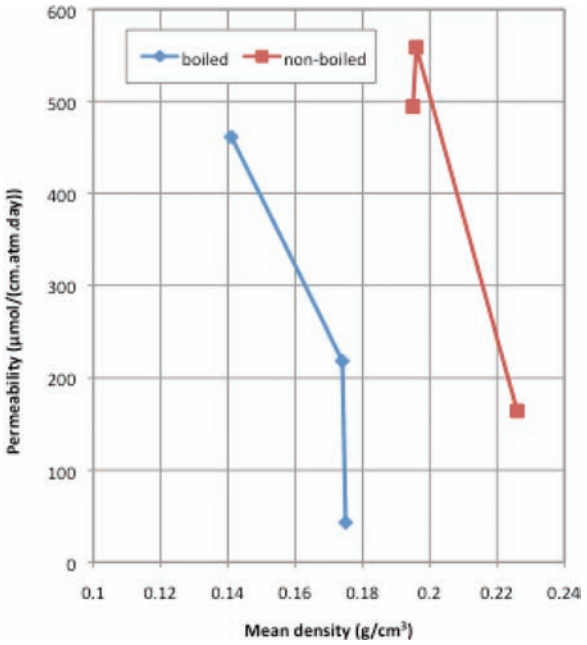

Figure 9. Permeability as a function of the density for data grouped per plank class as in Figure 4; the lower the density the higher is the mean permeability. Boiled samples showed a lower permeability than non-boiled samples, although having lower density.

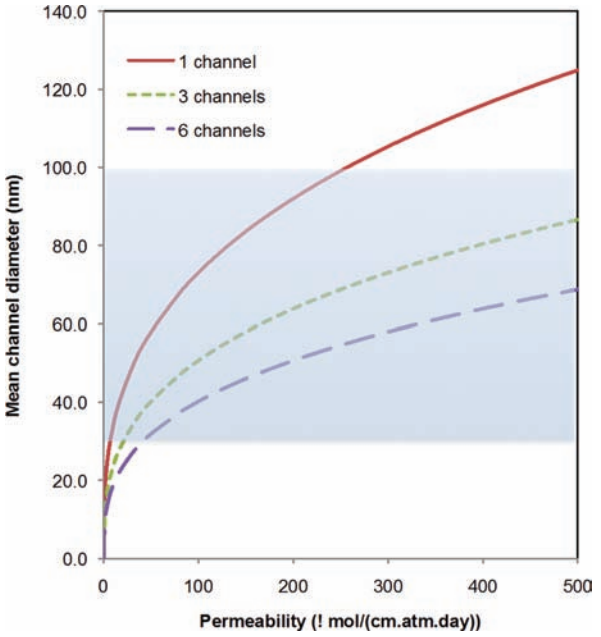

Figure 10. Range of channel diameters between cells as a function of the permeability. The diameters of 30−100 nm fit the range of permeabilities found in cork. Fits for one, three, and six channels per cell are shown.

channels can be roughly estimated from the measured flow rate through samples of known thickness. The gas flow through a restriction can be described in terms of a quantity known as conductance, *C*. This quantity describes the ease with which gas flows in such restrictions according to the following equation:

$$Q_{mol} = C_{eq} \times \Delta p_t$$

Here C_{eq} is the equivalent conductance of all the individual channels in a sample. Every sample can be described as a series of many single channels or conductances, these series being in parallel among them. If we take, in a rough approximation, all channels with the same diameter, one sample will have *n* channels in series and *m* series of channels in parallel. It can be shown that the equivalent conductance is then given by

$$C_{eq} = \frac{m}{n} C_i$$

with C_i the individual conductance for each channel. Combining the previous equations, we reach a relationship between the channel diameter and other quantities:

$$D^3 = \frac{L}{a} \times \frac{n}{m} \times \frac{Q}{\Delta p_t} \times \left(\frac{M}{T}\right)^{1/2}$$

Making the rough approximation of a cork cell to a cube of 30 μm per side, one can estimate how many cells are in a sample of known thickness and, therefore, how many individual conductances are in series and in parallel.

The channel length can be sought from the literature as the typical wall thickness, around 1.5 μm. Taking the gas flow shown in Figure 3 for sample 2B (7×10^{-6} mbar·L/s), we reach the diameter of 60 nm. This diameter was estimated assuming that there is only one channel between cells. For instance, if we consider three channels instead of one channel, we reach a mean diameter of 40 nm. Although this is a rough estimate, these values are in the range of diameters of plasmodesmata observed by electron microscopy crossing the cork cell walls.[9]

Figure 10 plots the diameter calculated by this process as a function of the permeability. The shaded area of 30−100 nm covers most of the measured permeability values. These calculations suggest that permeation through cork is essentially done by channels between cells and not through the walls or by other ways. The gas flow through solid cell walls should be much lower than by channels (for uncompressed cork).

Another relevant parameter in permeation measurements is the time lag as illustrated in Figure 3. Within the measured samples, the time lag ranged from 8 to 5680 s and did not correlate with the permeability. One could expect that the lower the permeability, the higher the time to achieve a constant flow. Although this was found in many samples, many others did not exhibit this behavior. This finding may suggest that some cells are completely closed or have smaller channels. This matches the electron microscopy observations on the variation of plasmodesmata distribution across cell walls.[9] Therefore, in such cells the time to achieve equilibrium with the permeant gas is much longer, leading to a delay in the steady state flow.

This work has allowed a comprehensive assessment of the permeability of different gases through uncompressed cork. A novel technique based on a helium mass spectrometer leak detector was successfully used to measure the permeability, providing a fast and quantitative measurement of the flow through a sample in a range of many orders of magnitude, being easily traceable to SI units.

Natural cork defects seemed to be not the major reason for the variability of permeability found by other authors in thick closures, because we found the same variability in thin selected samples. However, cork density and boiling processing are factors affecting the mean permeability.

The frequency distributions of permeability we measured (boiled and nonboiled) are not Gaussian, having a long tail to

high values. The mean permeability has a limited significance because it is several times the most probable value (mode).

The model of molecular transport through pores fits well to the measured data for different gases. Further calculations suggested that transport is made through small channels between cells, the plasmodesmata, with diameters that can range from 30 to 100 nm.

It should be stressed that these results were obtained for uncompressed cork and, therefore, cannot be directly applicable to cork closures. However, they provide a clear picture of the permeability of cork, as a natural material, to several gases.

Funding Sources

The financial support of the Portuguese Foundation for Science and Technology is gratefully acknowledged.

■ ACKNOWLEDGMENT

We thank Augusta Costa for cork plank characterization and Bobbie-Jean Shaw for the final English language revision.

■ REFERENCES

(1) Limmer, A. Do corks breathe? On the origin of SLO. *Aust. N. Z. Grapegrower Winemaker, Annu. Tech. Issue* **2005**, 89–98.

(2) Crochier, G. K. Measuring oxygen ingress during bottling/storage. *Pract. Winery Vineyard* **2007**, Jan/Feb, 1−6

(3) Mills, N.; Lopes, P.; Cabral, M. Oxygen brings new life to closure debate. *Aust. N. Z. Grapegrower Winemaker, Annu. Tech. Issue* **2006**, 112–114.

(4) Skouroumounis, G. K.; Kwiatkowski, M. J.; Francis, I. L.; Oakey, H.; Capone, D. L.; Duncan, B.; Sefton, M. A.; Waters, E. J. The impact of closure type and storage conditions on the composition, colour and flavour propoerties of a Riesling and a wooded Chardonnay wine during five years' storage. *Aust. J. Grape Wine Res.* **2005**, *11*, 369–377.

(5) Godden, P.; Francis, L.; Field, J.; Gishen, M.; Coulter, A.; Valente, P.; Høj, P.; Robinson, E. Wine bottle closures: physical characteristics and effect on composition ad sensory properties of a Semillon wine. 1. Performance up to 20 months post-bottling. *Aust. J. Grape Wine Res.* **2001**, *7*, 64–105.

(6) Lopes, P.; Saucier, C.; Teissedre, P. L.; Glories, Y. Main routes of oxygen ingress through different closures into wine bottles. *J. Agric. Food Chem.* **2007**, *55*, 5167–5170.

(7) Karbowiak, T.; Gougeon, R. D.; Alinc, J. B.; Brachais, L.; Debeaufort, F.; Voilley, A.; Chassagne, D. *Crit. Rev. Food Sci. Nutr.* **2010**, *50*, 20–52.

(8) Silva, S. P.; Sabino, M. A.; Fernandes, E. M.; Correlo, V. M.; Boesel, L. F.; Reis, R. L. Cork: properties, capabilities and applications. *Int. Mater. Rev.* **2005**, *50*, 345–365.

(9) Teixeira, R. T.; Pereira, H. Ultrastructural observations reveal the presence of channels between cork cells. *Microsc. Microanal.* **2009**, *15*, 1–6.

(10) Pereira, H. *Cork: Biology, Production and Uses*; Elsevier: Amsterdam, The Netherlands, 2007.

(11) U.S. Patent 6,561,008 B1, May 13, 2003

(12) Poças, M. F.; Ferreira, B.; Pereira, J.; Hogg, T. *Packag. Technol. Sci.* **2010**, *23*, 27–33.

(13) Limmer, A. The 'permeability' of closures. *Aust. N. Z. Grapegrower Winemaker, Annu. Tech. Issue* **2006**, 106–111.

(14) ASTM D-1434-82, Standard Test Method for Determining Gas permeability Characteristics of Plastic Film and Sheeting, 2003.

(15) Rutherford, S. W.; Do, D. D. Review of time lag permeation technique as a method for characterisation of porous media and membranes. *Adsorption* **1997**, *3*, 283–312.

(16) Mills, N. Sealing themes and variations. *Wine Ind. J.* **2005**, *20*, 52–58.

(17) Godden, P.; Lattey, K.; Francis, L.; Gishen, M.; Cowey, G.; Holdstock, M.; Robinson, E.; Waters, E.; Skouroumounis, G.; Sefton, M.; Capone, D.; Kwiatkowski, M.; Field, J.; Coulter, A.; D'Costa, N.; Bramley, B. Towards offering wine to the consumer in optimal condition − the wine, the closures and other packaging variables: a review of AWRI research examining the changes that occur in wine after bottling. *Aust. N. Z. Wine Ind. J.* **2005**, *20*, 20–30.

(18) Lopes, P.; Saucier, C.; Glories, Y. Nondestructive colorimetric method to determine the oxygen diffusion rate through closures used in winemaking. *J. Agric. Food Chem.* **2005**, *53*, 6967–6973.

(19) Lopes, P.; Saucier, C.; Teissedre, P. L.; Glories, Y. Impact of storage position on oxygen ingress through different closures into wine bottles. *J. Agric. Food Chem.* **2006**, *54*, 6741–6746.

(20) Hart, A.; Kleinig, A. *The Role of Oxygen in the Aging of Bottled Wine*; Wine Press Club of New South Wales: Australia, 2005; pp 1−14

(21) Silva, A.; Lambri, M.; De Faveri, M. D. Evaluation of the performances of synthetic and cork stoppers up to 24 months post-bottling. **2003**, *216*, 529−534

(22) Rosa, M. E.; Pereira, H.; Fortes, M. A. Effects of hot water treatment on the structure and properties of cork. *Wood Fiber Sci.* **1990**, *22*, 149–164.

(23) Pereira, H.; Graça, J.; Baptista, C. The effect of growth rate on the structure and compressive properties of cork. *IAWA Bull.* **1992**, *13*, 389–396.

(24) See, for instance, Chapter 4 of *Handbook of Vacuum Technology*; Jousten, K., Ed.; Wiley-VCH: Weinheim, Germany, 2009.